Applied Physics B (2021) 127:54
https://doi.org/10.1007/s00340-021-07593-x

Applied Physics B
Lasers and Optics

REGULAR PAPER

Passively Q-switched Cr:LiCAF laser with a saturable Bragg reflector

Serdar Okuyucu[1] · **Yusuf Ozturk**[1] · **Umit Demirbas**[1,2]

Received: 9 January 2021 / Accepted: 11 February 2021 / Published online: 19 March 2021

Abstract
We present a low-cost multimode diode pumped passively Q-switched Cr:LiCAF laser operating near 800 nm. AlGaAs-based saturable Bragg reflectors (SBRs) were used for passive Q-switching. The system is experimentally characterized in detail using four different output couplers and two SBRs with different modulation depths. Pulse widths in the 1.5–4 μs range at repetition rates between 18 and 40 kHz were achieved with average powers up to 125 mW. The experimentally obtained results are compared with basic Q-switching theory and further performance improvement in terms of pulse length shortening and peak power scaling is elaborated.

1 Introduction

Implementation of lasers with pulse widths in the nanosecond–microsecond range is desired for a variety of applications including range finding, nonlinear frequency conversion, material processing, and remote sensing [1]. Q-switching or gain switching techniques are usually employed in obtaining short, high-energy pulses with high peak powers. In Q-switching, intracavity loss of a laser resonator is modulated to produce pulsed output; whereas, gain-switched operation is based on pulsed pumping of the laser material with a pump pulse width in the order of the fluorescence lifetime of the gain material. In Q-switched operation, resonator losses can be modulated by the use of active or passive modulation schemes [2, 3]. In the implementation of actively Q-switched lasers, acousto-optic modulators, electro-optic modulators, or rotating mirrors with external driving circuitry are typically used, but these systems suffer from higher cost, lack of compactness, and increased complexity. On the other hand, implementation of passively Q-switched lasers is more economical, simple, and practical where cavity losses are modulated by the use of saturable absorbers, such as dye-based absorbers, Cr^{4+}:YAG (for 1μm lasers) [4], Cr^{2+}:ZnSe (for 1.5μm and 2μm lasers) [5], or SESAM/SBR-based nonlinear mirrors (semiconductor saturable absorber mirror [6]/saturable Bragg reflector [7]). However, in passive Q-switching, it is harder to provide independent control of parameters such as pulse shape, pulse energy, peak power, and pulse repetition rate.

Ti:Sapphire [8], Alexandrite [9], and Cr:Colquiriite crystals (Cr:LiSAF [10], Cr:LiCAF [11], Cr^{+3}:LiSGaF [12], and Cr:LiSCAF [13]) are among the favorable solid-state laser gain media that could generate broadly tunable Q-switched output in the ~ 700–1100 nm range and below (375–550 nm and 235–365 nm regions via frequency doubling/tripling [14–16]).

In this work, we focus our attention on Cr:Colquiriites, which attracted a renewed interest over the last two decades, due to the brightness improvement observed in LED (light-emitting diode) and laser diode pump sources. Strong electron–phonon coupling creates three intense and broad absorption bands in Cr:Colquiriite gain media that are centered around ~275 nm, ~445 nm, and ~640 nm [10, 17]. The 640 nm transition ($^4A_2$ to $^4T_2$ excitation) has a full-width-half-maximum (FWHM) approaching 100 nm, and it is strong both for the E//a and E//c axis in the uniaxial Cr:Colquiriite crystals. This broad absorption band facilitates direct-diode pumping of Cr:Colquiriites by low cost and well-developed AlGaAs- and AlGaInP-based diodes in the red spectral region. Additionally, at room temperature, Cr:Colquiriites have upper state fluorescence lifetimes (τ_f) that are ~20–50 times longer than that of Ti:Sapphire (67 μ*s* in Cr:LiSAF, 175 μ*s* in Cr:LiCAF, 3.2 μ*s* in Ti:Sapphire [18]). Moreover, unlike Alexandrite and Ti:Sapphire

✉ Serdar Okuyucu
serdar.okuyucu@antalya.edu.tr

[1] Laser Technology Laboratory, Department of Electrical and Electronics Engineering, Antalya Bilim University, 07190 Antalya, Turkey

[2] Center for Free-Electron Laser Science, Deutsches Elektronen Synchrotron, Hamburg 22607, Germany

that limit active laser ion doping levels below ~0.25%, Cr:Colquiriites could reach 100% doping without sacrificing too much from the crystal quality (e.g., LiChrom, $LiSrCrF_6$, 100% Cr doped $LiSrAlF_6$) [19]. This then ideally enables the achievement of large inversion densities that is quite important for efficient Q-switched lasing and amplifier operation. However, note that the fluorescence lifetime of the upper lying laser level depends on inversion density in Cr:Colquiriites due to the presence of Auger energy transfer upconversion (ETU) process [20]. On top of that, Cr:Colquiriites are also sensitive to temperature quenching of fluorescence lifetime; hence, a careful optimization of doping and thermal effects is required to achieve the desired performance [21]. Cr:Colquiriites possess moderate emission cross section (σ_{em}) values, but due to their longer fluorescence lifetime, the gain product ($\sigma_{em}\tau_f$) of Cr:Colquiriites is ~2–2.5 times higher compared to Ti:Sapphire. With the additional advantage of low crystal passive losses in Cr:Colquiriites, this results in relatively high slope efficiencies (above 50%) and one of the lowest lasing thresholds (sub mW) attained among solid-state lasers [22]. Combined with the performance shown in a number of previous studies such as sub-10-fs light pulse generation via mode-locking [23–25] and widely tunable laser operation (700–1100 nm) [16], these properties promote the construction of compact, low-cost and efficient Cr:Colquiriite lasers that can replace more costly Ti:Sapphire-based systems in a variety of applications.

Active and passive Q-switching of Cr: Colquiriites have been studied by several groups. Earlier systems were usually based on flashlamp pumping, where high-energy Q-switched pulses were obtained at the expense of very low repetition rate operation [14, 15, 26–29]. Due to the large gain available under flashlamp pumping, pulse energies were usually limited by the damage threshold of cavity optics in these systems. As an example, using a rotating mirror Q-switched Cr:LiSAF laser, Stalder et al. reported 50 ns pulses with 150 mJ energy at 1 Hz [26]. Using acousto-optic Q-switching, 20 ns pulses with 120 mJ energy at 1 Hz were achieved by Pinto et al. along with a broad tuning capability covering the 780–1065 nm range [14, 15]. Using V:YAG [27] and Cr:YSO [28] as passive Q-switching elements, 1 mJ level 50 ns long pulses at 2 Hz and 45 ns pulses with 7.5 mJ energy were obtained from flashlamp-pumped Cr:LiCAF systems. Klimek et al. attained up to 0.5 J energies at 5 Hz with around 1–1.5 µs pulse widths from a thin-slab Cr:LiSAF laser [30]. Interestingly, Weber et al. observed 180 ns pulses with 60 mJ energy from a self-Q-switched Cr:LiSAF laser [31, 32]. The thermal effects limited the operation frequencies in these flashlamp-pumped systems, and direct diode pumping could enable a solution route for this. From diode-pumped systems, 230 ns pulses with 6.5 J at 10 kHz (Cr:LiSAF) [33, 34], 250 ns with 6.5 J at 10 kHz (Cr:LiSGaF) [35] were reported via acousto-optic Q-switching. Self-Q-switched operation with 5 s long pulse widths with 2 J energy at around 20 kHz was realized from a low-power single-mode diode-pumped Cr:LiCAF laser system [36]. Recently, 42 ns 140 µJ pulses were achieved at 10 Hz from a Cr:YAG Q-switched Cr:LiSAF laser pumped by LEDs [37]. We see that, in diode/LED pumped systems, one can achieve high repetition rate operation, but pulse energies are then quite low (due to the thermal limits which hinder realizable average powers).

In this paper, to our knowledge, we report the first passive Q-switching experiments of Cr:LiCAF with saturable Bragg reflectors (SBRs). Usage of SBRs for passive Q-switching potentially enables control of key behavioral characteristics of the Q-switched laser by carefully optimizing SBR properties such as modulation depth, saturation fluence, and recovery time. Among Cr:Colquiriites, we focused our attention to Cr:LiCAF crystal due to its superior thermomechanical strength and long upper state fluorescence lifetime [16]. The Cr:LiCAF laser is pumped by two low-cost 665 nm broad-area laser diodes, which provided a total pump power of 3.6 W. In cw experiments, an output power level up to 470 mW (with 15% efficiency) was available around 800 nm. Q-switching was initiated and sustained by the use of two different AlGaAs-based SBRs with different modulation depths and laser performance was investigated at different levels of output coupling. In Q-switched operation, the laser produced pulses down to 1.62 µs near 800 nm with an average power of 127 mW. The repetition rate varied between 18 and 40 kHz with pulse energies up to 3.5 µJ and peak powers up to 1.9 W around 800 nm. The observed pulse widths are relatively long and the achieved peak powers are relatively low in this initial study, and possible solution paths will be discussed as we present the experimental results in detail. The paper is organized as follows: Sect. 2 describes the experimental setup used in cw and Q-switched laser studies and provides details on the AlGaAs-based SBR that is used for passive Q-switching. In Sect. 3, we present the Q-switching results in detail and discuss performance parameters for different output couplers, SBRs, and pump power levels. We finalize with Sect. 4 with a brief discussion, where we also elaborate on possible ways to improve the results obtained in this initial study.

2 Experimental setup

Figure 1 shows a schematic description of the diode-pumped Cr:LiCAF laser cavity that is used in both continuous wave (cw) and Q-switched laser experiments. Two linearly-polarized single-emitter multi-mode diodes (MMD-1 and MMD-2) each of which can provide 1.8 W at a maximum drive current of 2.3A were used as pump

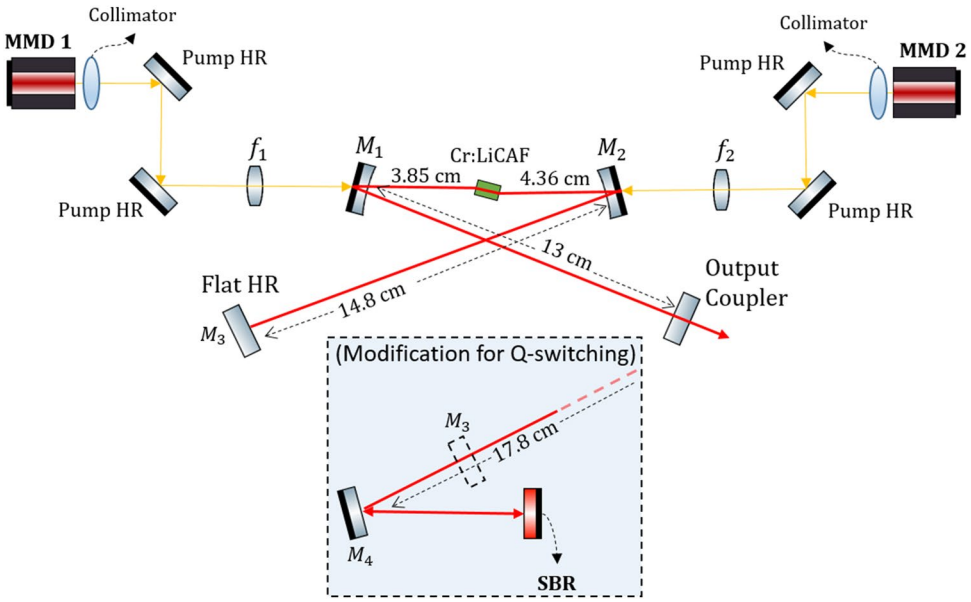

Fig. 1 Experimental setup of the multi-mode diode (MMD) pumped Cr:LiCAF cavity for cw and Q-switched lasing experiments. *SBR* Saturable Bragg reflector, *HR* High reflector

sources. The single emitter MMD diodes had an asymmetric transverse emitting area of 1 µm × 150 µm. The diode output was diffraction-limited along the fast axis and multimode along the slow axis with an M^2 value of approximately 10. A built-in cylindrical micro-lens partially collimated the diode beam in the fast axis. Later on, the output of the laser didoes was further collimated with aspheric lenses of focal length of 4.5 mm and then focused inside the laser crystal by the use of achromatic doublets with focal lengths of 75 mm (f_1,f_2). The gain material was a 5 mm long, 4 mm wide, and 1.5 mm thick piece of Cr:LiCAF crystal with 7 mol. % chromium doping. The Cr:LiCAF sample had Brewster–Brewster cut surfaces, and the E//c axis is employed in lasing experiments. The crystal absorbed ~98.3% of the TM polarized pump light. Taking the losses at the lens and dichroic mirrors into account, around ~94.7% of the power available from the diodes was absorbed by the crystal. The Cr:LiCAF crystal was mounted in a copper holder with indium foil around it and water cooling was used to keep the crystal boundary temperature at 15 °C.

The Cr:LiCAF laser resonator was a standard x-folded, astigmatically compensated cavity consisting of two curved dichroic pump-mirrors (M_1, M_2), with radius of curvatures (roc) of 75 mm, a flat end high reflector (M_3), and a flat output coupler (OC). Dichroic mirrors (M_1 and M_2) had reflectivity greater than 99.9% in the 730–910 nm wavelength range and had >98% transmission in the pumping window. The short and long cavity arm lengths were around 13 cm and 14.8 cm, respectively. A resulting laser mode area (A) of ~ π 56µm ×42 µm was obtained inside the Cr:LiCAF crystal. The temporal and spectral characteristics of the cw laser setup were investigated using 4 different output couplers with transmission grades of 0.35%, 0.7%, 1.6%, and 2.75%. The round-trip travel time (T_R) of the cw cavity was around 2.5 ns.

In Q-Switching experiments, SBRs were used for initiating and sustaining Q-switched pulsing. During trials, the initiation of Q-switching was not possible by direct replacement of M_3 by the SBR, thus, following the extraction of M_3, a 150 mm radius of curvature mirror (M_4) was used to generate a secondary focus where we have placed the SBR (shown within the dashed box in Fig. 1). This focus (~70–100 m) was tight enough to initiate Q-switching, but not too tight to prevent mode-locking (or Q-switched mode-locking). Figure 2 shows the physical structure of the SBR that is used in this work. The SBR consists of 26 pairs of AlAs-$Al_{0.17}Ga_{0.83}As$ quarter-wave layers as the Bragg stack to provide high reflectivity at a central wavelength of 800 nm. The SBR contains five 6 nm thick GaAs quantum wells (QWs) sandwiched between $Al_{0.17}Ga_{0.83}As$ barriers for the saturable absorber action. The estimated absorption band edge of the QW is around 835 nm. The mirror–absorber combination is implemented on top of a GaAs substrate.

To obtain SBRs with different modulation depths and saturation fluences, we have used one or two pairs of SiO_2 and TiO_2 as an additional high reflective (HR) coating layer (Fig. 2 shows the case with 1 pair of coating). Figure 3 shows the calculated small signal and saturated reflectivity curves for the 800 nm SBRs with no coating (regular), 1-layer-HR coating and 2-layer-HR coating. As it can be seen from Fig. 3, incorporation of additional HR layers to the SBR structure decreases the modulation depth and increases the reflectivity bandwidth of the SBR (as a result, the saturation fluence also increases) [38, 39]. To be more specific, the designed/estimated modulation depths of the

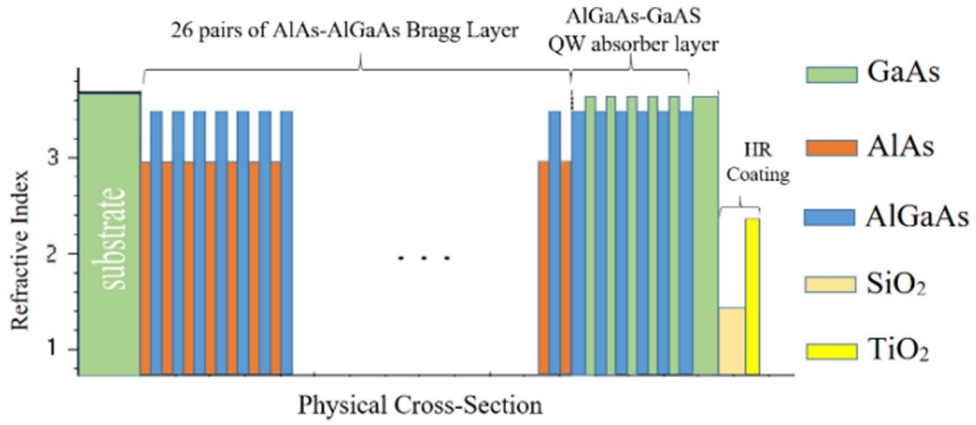

Fig. 2 Refractive index profile and physical thickness of each layer for the 1-layer-HR-coated 800 nm SBR that is used in this study (dimensions not to scale). The Bragg layers have an optical thickness of 200 nm ($\lambda/4$), and have a corresponding physical thickness of 66.55 nm and 57.15 nm for the AlAs and $Al_{0.17}Ga_{0.83}As$, respectively. The structure contains five 6 nm thick GaAs quantum wells, a 5 nm GaAs cap to prevent oxidization, and an additional SiO_2/TiO_2 quarter-wave pair high reflector to improve the overall reflectivity of the SBR

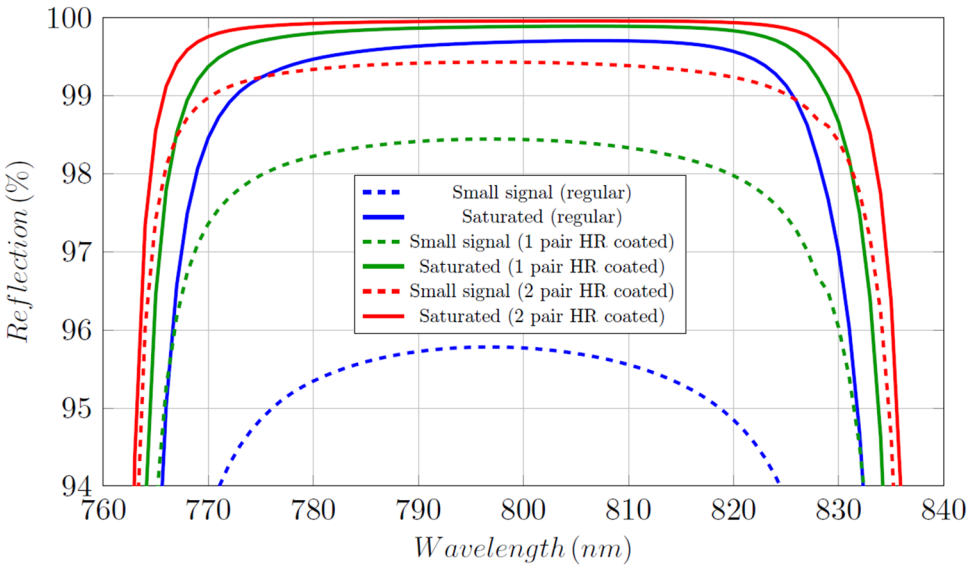

Fig. 3 Calculated small signal and saturated (large signal) reflectivity curves for the uncoated, one-layer-HR-coated and two-layer-HR-coated 800 nm SBRs. Details of the design are presented in Fig. 2

SBRs were around 4.2%, 1.4%, and 0.5% for the regular, 1-pair-HR-coated and 2-pair-HR-coated SBRs, respectively. The uncoated SBR had a measured modulation depth of 4.5%, which confirms that the structure is grown close to its design specifications. Moreover, the uncoated SBR had a measured saturation fluence of 35 μ J/cm^2, a two-photon starting fluence of 2mJ/cm^2, and a decay time of around 20 ps. Note that, the modulation depth of the uncoated SBR (4.5%) was too high for the low-gain Cr:LiCAF laser material. Hence, in our experiments, we have only used the HR-coated SBRs with 0.5% and 1.4% modulation depths in our Q-switching trials.

In the experiments, to obtain the Q-switched output, the distance between the SBR and M_4 was scanned carefully by changing the position of the SBR over a range along the beam axis where lasing was present (along the stability range of the cavity: adjusting the SBR and M_4 distance enabled fine tailoring of the spot size radius on the SBR between 70 and 100 μm). Within this range, for a given OC, similar temporal Q-switching behavior (pulse shape, pulse-width, and repetition rate) was observed at a number of different locations of the SBR along the beam axis. Among those operation points, for each OC, we have chosen the location where the Q-switched laser average power was highest. Stable Q-switched operation was obtained with different output couplers having transmissions of 0.35%, 0.7%, 1.6%, and 2.75%. Detailed Q-switched data were taken during the experiments and main parameters

such as pulse-width, repetition rate, average output power, optical spectrum, RF spectrum, and beam profile were recorded.

3 Experimental results and discussion

3.1 Continuous-wave lasing results

In cw experiments, the position of the laser crystal, pump focusing lens, and the cavity alignment were all optimized as in Fig. 1, as to obtain the maximum power output around 800 nm at a certain pumping power from both diodes. The power efficiency curves for each one of the 0.35%, 0.7%, 1.6%, and 2.75% OCs were then constructed by operating both diodes simultaneously at the same discrete levels of input current. A maximum total pump power of 3.57 W was available at the maximum current of 2.3 A for both diodes.

Figure 4a shows the measured cw power efficiency curves for the Cr:LiCAF laser. By comparison, 0.7% OC is seen to provide the best results where output powers up to 468 mW was achieved at 3.5 W of absorbed pump power. The corresponding lasing threshold and slope efficiency with respect to absorbed pump power were 390 mW and 14.8%, respectively. The lasing threshold was measured lowest (190 mW) with 0.35% OC and is seen to increase (up to 1090 mW for 2.74% OC) for increasing levels of output coupling. The measured slope efficiencies of the current work (14.8% max) are significantly lower than the intrinsic and reported efficiency of ~60% of the Cr:LiCAF laser (obtained via Ti:Sapphire pumping) [40]. Some of this is due to the difficulty of mode-matching to the multimode pump beam. On the other hand, a cw slope efficiency of 32% [40] and 49% [41] were reported in similar MMD diode-pumped systems, while using a 10% Cr-doped LiCAF sample with ~0.3% passive loss and 5% Cr-doped LiCAF sample with ~0.1% passive loss, respectively. The relatively highly Cr-doped (7%) LiCAF sample in our study had an internal crack from earlier power scaling studies, and we believe that this increased the passive losses of the sample at hand to around 0.6%. Unfortunately, no other sample was available during this study; however, since we focused on understanding the potential of Q-switched Cr:LiCAF lasers in this initial work, this does not significantly change the results that will be presented in the next section (except the obtainable average power levels, which could be scaled further in future studies by employing lower-loss Cr:LiCAF samples).

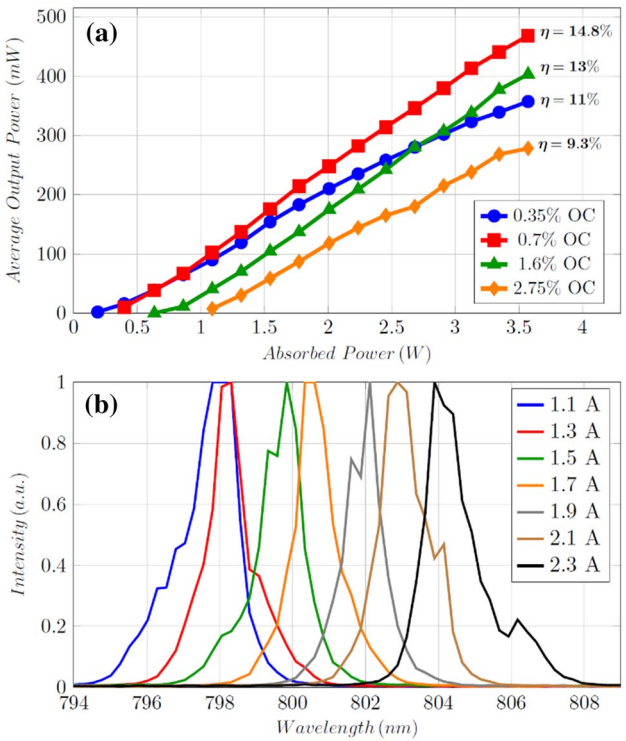

Fig. 4 **a** Power efficiency data of the continuous-wave Cr:LiCAF laser taken with four different OCs with transmission in the range from 0.35 to 2.75%. **b** Measured optical spectrum of laser with 0.7% OC at different levels of diode current or pump power (0.85 W at 1.1 A, 3.5 W at 2.3 A)

Figure 4b shows sample optical spectra obtained from the cw Cr:LiSAF laser, where we see variation of laser wavelength with pump current for the 0.7% transmitting output coupler. As we can see from Fig. 4b, the free-running optical spectra of the cw Cr:LiCAF laser were centered around 800 nm and had a FWHM of ~1.8 nm. A clear shift of laser central wavelength from 798 nm and 804 nm is easily visible as the pump diode current is increased from 1.1 to 2.3 A (corresponding absorbed pump powers increase from 0.85 to 3.5 W). The observed laser wavelength drift is due to the shift of emission gain peak to longer wavelengths with increasing temperature of the crystal.

3.2 Q-switched lasing results

We start the presentation of our Q-switched lasing results with Fig. 5, which shows the variation of measured output power with absorbed pump power level. The data are taken using: (1) 1-layer-HR-coated SBR and 0.35%, 0.7%, 1.6%, and 2.75% transmitting output couplers, and (2) 2-layer-HR-coated SBR with the 0.7% transmitting output coupler. Comparing Fig. 5 with the earlier cw performance (Fig. 4), we see that, in Q-switched experiments, the achievable laser slope efficiencies decreased significantly: highest efficiency is 7% for 0.7% OC in comparison to the 14.8% observed in cw operation due to the additional losses associated with the SBR. Note that, on purpose we did not employ a very tight focus on the SBR (to prevent mode-locking), and as a result, the increase of cavity losses not only includes non-saturable

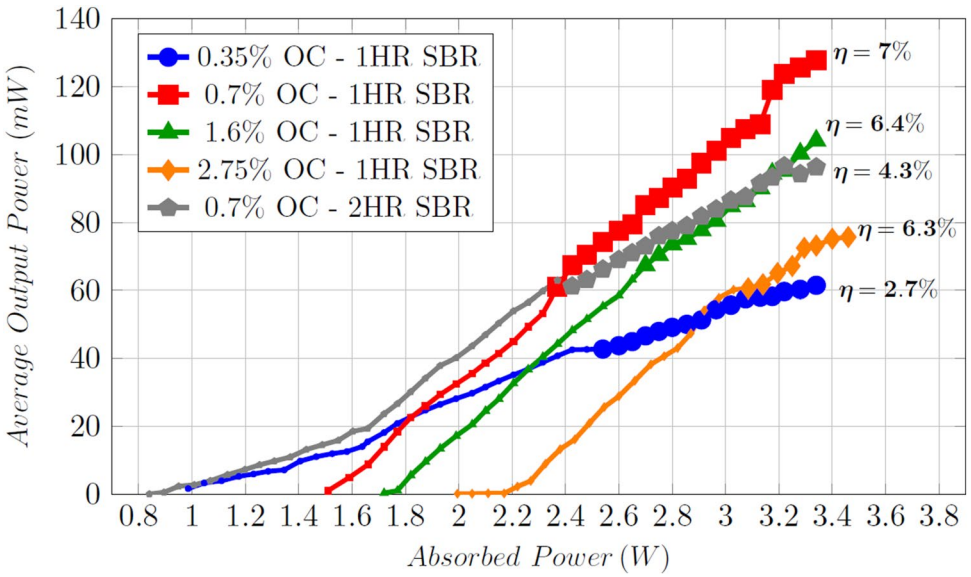

Fig. 5 Measured power efficiency data of the SBR Q-switched Cr:LiCAF laser taken with four different OCs with transmission in the range from 0.35 to 2.75%. 1HR SBR: 800 nm SBR with one additional pair of HR coating, 2HR SBR: 800 nm SBR with two additional pairs of HR coating

losses of the SBR, but also some portion of the saturable losses, as the SBR was not fully saturated in this study.

With the one-layer-HR-coated SBR, the highest average power was obtained using the 0.7% output coupler: around 125 mW at around 3.4 W absorbed pump power level. When we compare the results obtained with one and two-layer-HR-coated SBRs (both taken with the 0.7% OC), a lower lasing threshold is obtained with the 2HR-SBR as expected (due to lower overall losses). On the other hand, the maximum average power obtained was only 100 mW, probably due to the additional difficulty in bleaching the absorber hidden behind 2 HR coatings.

During the Q-switching experiments, cw regime was first observed at low absorbed pump power levels (shown with small markers in Fig. 5) and stable Q-switched operation (shown with larger markers) started only after absorbed pump power reached a certain value (a different level for each OC). This observation points to the requirement of a certain intracavity power level for the laser to reach a stable Q-switching operation. The interpretation of this behavior can be made based on the Q-switching condition given as [6],

$$\text{Q-Switching:} \left|\frac{\mathrm{d}R}{\mathrm{d}I}\right| I > r\frac{T_R}{\tau_f}, \tag{1}$$

where r is the pump parameter that is the ratio of pump power to the threshold pump power describing how many times the laser is pumped above threshold, T_R is the cavity round-trip time, τ_f is the upper state lifetime of the laser material, $\mathrm{d}R/\mathrm{d}I$ is the variation of SBR reflectivity with intensity and I is the laser intensity incident on the absorber. As nicely described in [6], left-hand side of Eq. 1 describes the loss reduction per cavity round-trip due to the saturation of the SBR, which increases the intracavity laser intensities. To compensate for this increase, the gain should saturate fast enough to reach a balance (right-hand side of Eq. (1)), and if the gain cannot catch up, a Q-switched pulse will evolve. It is clear from Eq. (1) that Q-switching tendency increases with increased upper state lifetime of the gain media, and among Cr:Colquiriites, Cr:LiCAF which has the longest room-temperature fluorescence lifetime (τ_f = 175µs) is an ideal candidate for Q-switching applications. Note also that, lasers with shorter cavities with smaller round-trip times (T_R) also have a higher tendency for Q-switching. Finally, a larger slope ($\mathrm{d}R/\mathrm{d}I$), a larger change of reflectivity with intensity (a smaller saturation fluence) also increases Q-switching tendency, as well as the Q-switched pulse build-up time [6].

We see from Eq. (1) that, with increasing pump power, the intracavity laser intensity and r will increase, whereas ($\mathrm{d}R/\mathrm{d}I$) will decrease due to SBR saturation and τ_f will potentially also decrease slightly due to increased inversion and crystal temperature. Overall, the increase of intracavity intensity dominates, and as the pump powers increase slowly, at one point the laser will start to Q-switch (of course, depends on all the other specifications of the system). We clearly see this behavior in our experimental data shown in Fig. 5. The laser first operates in pure cw regime with all output couplers: indicating that, the intensity fluctuations could easily be balanced. As the pump powers and intracavity laser powers increase, stable Q-switching is observed in all cases. We have also seen that, the required pump power level for Q-switching increases with increasing output coupling. This is a quite expected result, since the intracavity laser powers decrease with increasing output coupler transmission, and larger laser output powers (or pump powers) are required to reach the Q-switching point.

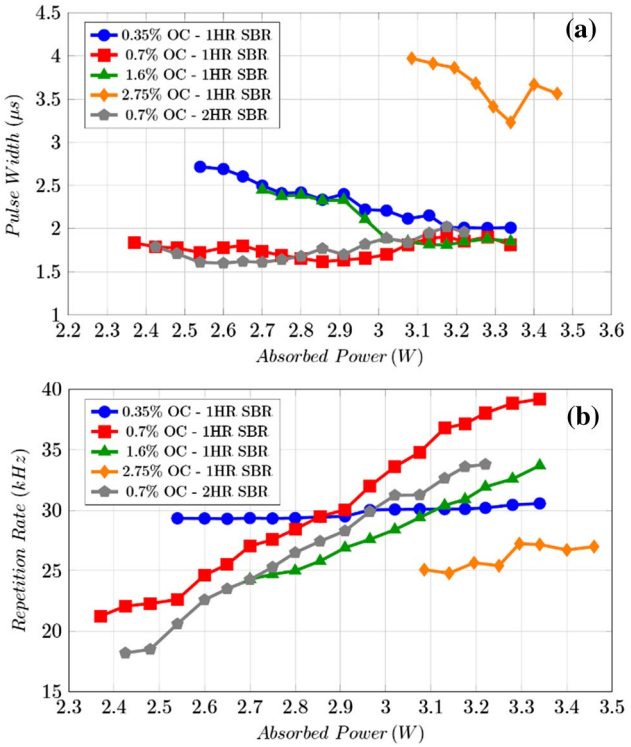

Fig. 6 Measured variation of **a** pulse-width and **b** repetition rate of the Q-switched Cr:LiCAF laser with absorbed pump power amount. The data are taken using different output couplers in the 0.35–2.75% range. 1HR SBR: 800 nm SBR with one additional pair of HR coating, 2HR SBR: 800 nm SBR with two additional pairs of HR coating

Figure 6 shows the measured variation of Q-switched Cr:LiCAF laser output pulse width and repetition rate with absorbed pump power. The data are taken with various output coupler values. During measurements, temporal waveform was recorded on a digital oscilloscope from which repetition rate values were readily available (eg. see Fig. 7). The output of the laser was also simultaneously monitored using an RF spectrum analyzer to confirm the stability of Q-switching. A sample plot of RF spectra is given in Fig. 8, which shows a clean peak with no side lobes at the repetition frequency of the Q-switched pulses (around ~31.8 kHz for this sample case). Note that, the Q-switching data are taken in an open laser setup, and it is clear that, the RF peak shown in Fig. 8 could be narrowed down further, by closing the laser cavity and by employing better temperature stabilization to the system. Also, for a more accurate determination of the laser pulse width from the measured oscilloscope trace, the two-dimensional pulse train data were subjected to an algorithm where the difference between the mid-crossings in between low and high state levels (FWHM) of the pulses were calculated and state levels were estimated by a histogram method, and reported values in Fig. 6a are average pulse width values (average pulse width of all the pulses that fit into a 2 ms window: ~ 40–80 pulses depending on the repetition rate).

If we start the discussion with the measured pulse widths, we see from Fig. 6a that, the pulse widths measured with the 0.7% OC stayed around 1.75 μs, showed some oscillation (±0.25 μs), but did not show a clear increasing/decreasing trend with changing absorbed pump power level (both for the 1HR SBR and 2HR SBR). For the 0.35% and 1.6% OC, we see a slow decrease of measured pulse widths from around 2.5–2.75 to 1.85–2 μs level. The data with the 2.75% deviate from others, where we have measured pulse widths of around 3.65 μs (a slight decrease of pulse widths from 4 to 3.5 μs level is also observable for this OC).

When we look at Fig. 6b, we see that for all cases the measured Q-switched repetition rate of the Cr:LiCAF laser increases almost linearly with absorbed pump power amount. However, note that the observed slope (rate of increase of repetition rate with the change of absorbed pump power) is quite different. As an example, for the 0.7% output coupler, the repetition frequency is seen to vary from around 21.2 kHz up to 39.2 kHz when the absorbed pump power was increased from 2.4 to 3.35 W. On the other hand, for the 0.35% OC, the repetition frequency only increases from 29.3 to 30.6 kHz for a similar pump power change.

It is educational at this point to try to understand the observed trends in Q-switched repetition rate and pulse width. For a fully saturated SBR, the pulse width (FWHM) of an SBR Q-switched laser can roughly be estimated using:

$$\tau_p = \frac{2\ln(2)T_R}{q_0}, \tag{2}$$

where q_0 is the saturable loss coefficient of the absorber (also known as modulation depth) [42]. The above formalism in Eq. (2) assumes that the growth rate and the decay rate of the Q-switched pulse are both q_0/T_R. Taking the decrease in growth and decay of the pulse during saturation of the gain (during rise and fall times) into account, a closer approximation could also be made by multiplication of Eq. (2) by another factor ~2.5 that gives [42, 43]:

$$\tau_p = \frac{3.52T_R}{q_0}. \tag{3}$$

For our case, for the experimental setup shown in Fig. 1, we had a round-trip cavity time (T_R) of around 3 ns, and for the 1-pair-HR-coated SBR, the calculated modulation depth $q_0 = \Delta R$ is around=1.4%, resulting in an estimate of the FWHM of the Q-switched pulses as $\tau_p = 0.7\mu s$. For the 2-pair-HR-coated SBR, the calculated modulation depth is around 0.5%, and this results in pulse width estimate of around 2.1 μs. Note that our measured pulse widths with the 1HR SBR are around 2–3 times longer than the simple

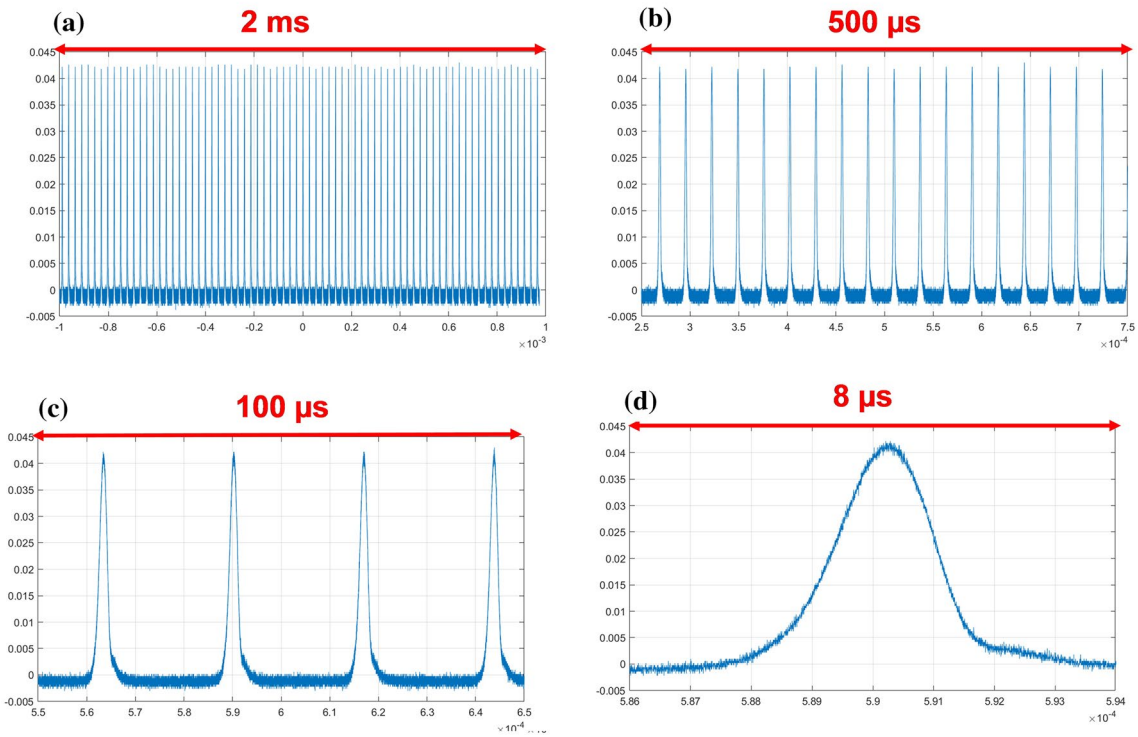

Fig. 7 Measured time dynamics of the Q-switched Cr:LiCAF laser in different time scales: **a** 2 ms, **b** 500 µs, **c** 100 µs, **d** 8 µs. The data are taken using the 0.7% OC with 1-layer-HR-coated SBR at an absorbed power of 3.13 W, while the Q-switched Cr:LiCAF laser output power was 109 mW. The pulse width and repetition frequency were 1.82 µs and 36.8 kHz respectively

estimate. We believe this is potentially due to the full-bleaching assumption made while driving Eq. (3); since in our case, we have on purpose did not use a tight focus on the SBR to prevent mode-locking (and hence our SBRs were clearly not fully bleached in our study). Moreover, if we look at the experimental data a bit closer, as expected from Eq. (3), the pulse width data with the 0.7% OC do not change with absorbed pump power level. On the other hand, the observed slow decrease of pulse width with pump power for the 0.35%, 1.6% and 2.75% OCs shows a sign of increased level of saturation of the SBR.

Regarding the repetition rate of Q-switched pulses at the output, a theoretical approximation for the repetition frequency can be formulated as in Eq. (4) provided that the repetition rate is much greater than the upper state lifetime τ_f of the laser (i.e. $f_{\text{rep}} \geq 2/\tau_f$) [44]:

$$f_{\text{rep}} \cong \frac{g_0}{2\Delta R \tau_f}. \tag{4}$$

In Eq. (4), g_0 is the small-signal gain coefficient with $g_0 = rL$ where r is the pump parameter (same as defined in Eq. (1)) and L is the total round-trip losses of the cavity including the saturable and non-saturable losses of the SBR, losses of the laser crystal and cavity optics as well as the effective loss of output coupling. Since g_0 varies approximately linearly with the pump power for a four-level laser system, one expects a linear increase of repetition rate with absorbed pump power level, and hence generally speaking, the experimentally measured trends in Fig. 6b comply with the theoretical expectations. However, as mentioned earlier, the rate of increase of repetition rate with the change of absorbed pump power is quite different for each OC, and it is especially relatively low for the 0.35% and 2.75% output couplers. For these OCs, the laser efficiencies were rather low (Fig. 9), and the system was operating further away from fully saturated absorber approximation, which might be the reason for the observed behavior. If we look at the case of 0.75% OC data in detail, using the 1-pair-HR-coated SBR, we have measured a lasing threshold of around 1.5 W. Stable Q-switching were obtained for absorbed pump powers levels between 2.4 and 3.35 W, with corresponding r values of around 1.6 and 2.23, respectively. When we look at the repetition rate data, we see an increase in the repetition rate from 21.2 to 39.2 kHz. The calculated increase in r value ~ 1.4 (~2.23/1.6) is considerably smaller than the measured increase in repetition rate ~1.85 (39.2/21.2), which demonstrates that Eq. (4) only roughly estimates the observed trend in our case, probably due to the simplifying assumptions used in its derivation.

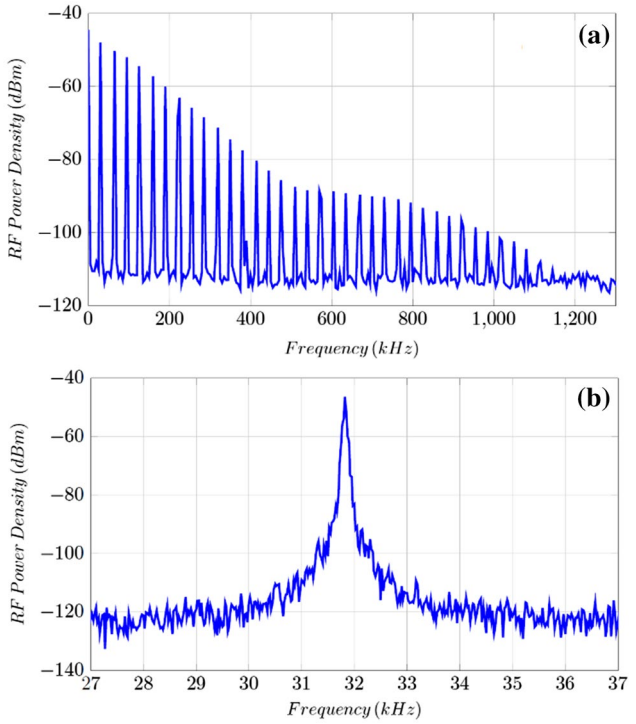

Fig. 8 Sample radio frequency spectrum of the Q-switched pulse train emitted from the Cr:LiCAF laser taken at different central frequencies: **a** RF centered at baseband with a span of 4 MHz, and resolution bandwidth of 100 Hz (only the positive frequencies are shown for better visibility). **b** RF centered at the Q-switching frequency around 31.8 kHz, with a span of 20 kHz, and resolution bandwidth of 10 Hz. The data are taken using the 0.35% OC with 1-layer-HR-coated SBR at an absorbed power of 3.13 W, while the Q-switched Cr:LiCAF laser output power was 58 mW. The pulse width and repetition frequency were 2.15 µs and 31.8 kHz respectively

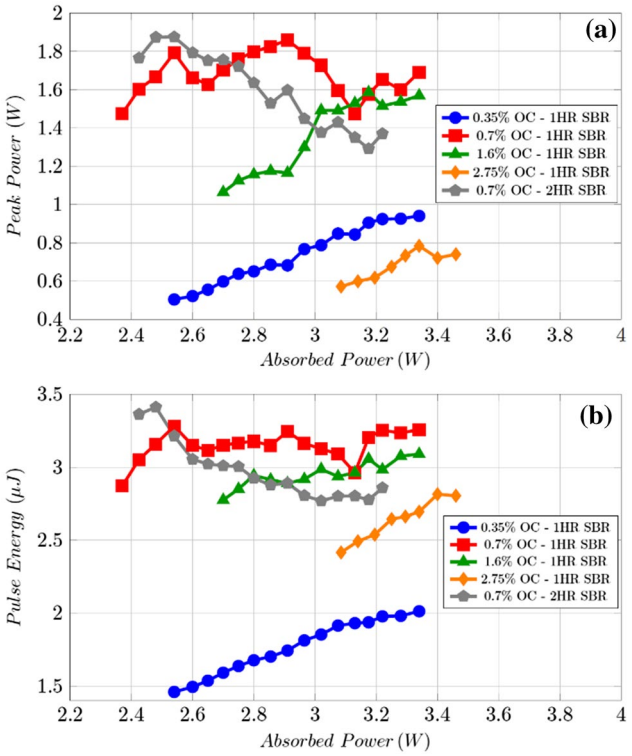

Fig. 9 **a** Peak power and **b** Pulse energy of Q-Switching laser with 1HR SBR and four different OCs. (including an additional trial for 2HR SBR with 0.68% OC)

Figure 9 shows the corresponding calculated peak powers and the pulse energies of the Q-switched Cr:LiCAF laser based on measured average output power (Fig. 5) and pulse width & repetition rate (Fig. 6) data. We see that there is some fluctuation in the calculated data in terms of variation of the measured parameters with absorbed pump power level. In terms of pulse energy, for the 0.7% and 1.6% output couplers, we do not observe any significant variation of energy with pump power. On the other hand, a slow increase in pulse energy could be seen in the data taken using 0.35% and 2.75% output couplers. Note that, peak powers up to ~1.9 W were obtained for 0.7% OC, thus the peak power of the laser is only scaled up to around four times in comparison to cw output. Calculated pulse energies are also around 3 µJ for most cases, except for the 0.35% OC, where the pulse energies were limited in the ~1.5–2µJ range.

It is again helpful to compare the measured data with theoretical estimations. A derivation of an equation for the pulse energy in a passively Q-switched laser using semiconductor saturable absorbers based on the reduction of gain during the evolution of pulse results in [42]:

$$E_p = E_l(2q_0)\frac{T_{\text{oc}}}{T_{\text{oc}} + L}, \tag{5}$$

where T_{oc} is the output coupler transmission, L is again the total round-trip cavity losses, and E_l is the saturation energy of the gain medium:

$$E_l = \frac{h\nu_l}{2\sigma_{\text{em}}}A. \tag{6}$$

Above, $h\nu_l$ is the laser photon energy, A is the laser mode area. According to Eq. (5), assuming a constant laser mode area, the pulse energy is expected to be independent of the pump power applied to the cavity (assumption of constant mode-area might not be fully valid in our case due to the variation of pump laser beam profile with diode current). As discussed above, some of the data taken match this expectation; whereas in some, we see some fluctuations, which might be again an indication of not fully saturated SBR operation regime or due to the unintended change in other laser parameters. For a more direct comparison of experimental findings with that of Eq. (5), the theoretical estimate of pulse

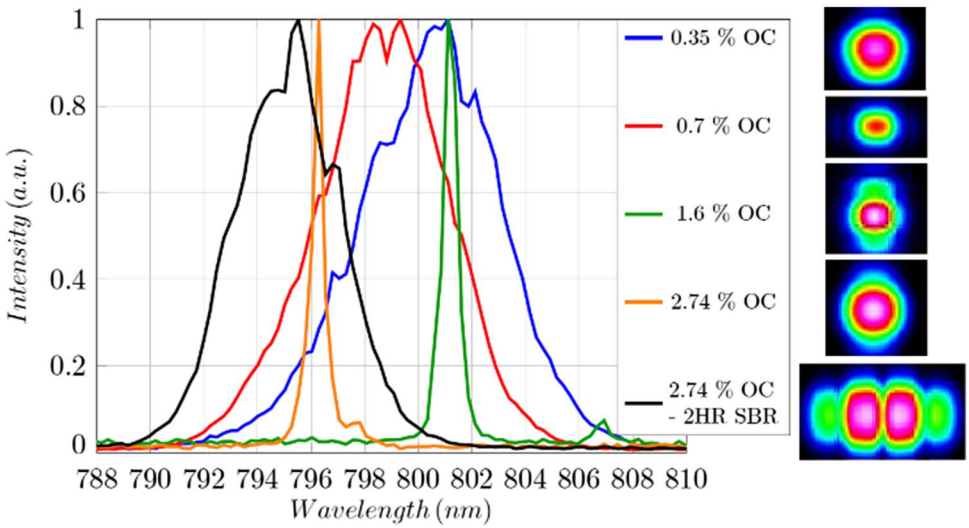

Fig. 10 Optical spectrum of Q-Switched Cr:LiCAF laser taken with 1-HR-coated and 2-HR-coated 800 nm SBRs at different output coupling levels. The inset picture shows the measured beam profile for each case

energy was made for the setup with 1-pair-HR-coated SBR (ΔR=1.4%) and 0.7% OC, where the calculation of E_p with the parameters of $\sigma_{em} = 1.3 \times 10^{-20}\text{cm}^2$, $A = \pi 56 \times 42\mu\text{m}^2$, and $L \sim 2\%$ is around 5.5μJ. This is 1.5–2 times above what is measured experimentally, and we again believe this might be mostly due to the full SBR saturation assumption made while deriving Eq. (6).

To finalize the subsection, sample optical spectra from the Q-switched Cr:LiCAF laser is shown in Fig. 10. Sample output beam profile data is also shown as an inset picture for each output coupler. When we look at the optical spectra, we see that, compared to cw operation (with spectral width ~1.8 nm), weak spectral widening (up to ~4 nm for 0.36% and 0.68% OC) and narrowing (down to ~1 nm for 1.6% and 2.74% OC) could be observed in the Q-switched case. Thus, we can say that the optical spectrum of the Q-switched pulses gets narrower with increasing output coupling, probably due to decreased overall net gain. When we look at the beam profile, we see that one mostly gets a TEM_{00} output despite the multimode pump beam due to relatively higher losses of the system which prevent lasing of the higher-order modes. As an exception, the laser output obtained with the 2-HR-layer-coated SBR was multimode, probably due to the lower overall losses of this SBR.

4 Conclusion

We have investigated passive Q-switched operation of a diode-pumped Cr:LiCAF laser using AlGaAs based SBRs for the first time. In cw laser experiments, around 0.5 W of output power with a slope efficiency of around 15% was reached. In Q-switched operation, the laser produced pulses down to 1.62 μs near 800 nm with an average power of around 125 mW. The repetition rate varied between 18 and 40 kHz with pulse energies up to 3.5 μJ and peak powers up to 1.9 W around 800 nm. Clearly, the obtained pulse widths with SBR Q-switching are rather long, compared to earlier passive Q-switching experiments with V:YAG [27], Cr:YSO [28], and Cr:YAG [37]. The peak power scaling of the system is also only three–fourfold compared to cw operation, partly due to the long pulse widths, and partly due to the relatively high losses of the SBR at hand.

We believe that, in future studies, shorter pulse widths could be achieved from SBR Q-switched Cr:LiCAF lasers by employing more compact cavities with reduced cavity round-trip time (Eq. 3). An SBR with a larger modulation could also be used to reduce the obtainable pulse widths. However, higher modulation depths will only be feasible in a system with improved gain, which could be achieved by using a lowly Cr-doped Cr:LiCAF sample (1–3%) with lower passive loss and reduced thermal issues. As described in [41], a lower Cr-doping could facilitate the usage of higher pump power levels via better distribution of heat load along the crystal length, which can then allow usage of an SBR with a larger modulation depth.

Note also that the usage of shorter cavities also reduces the mode-locking tendency of the SBR: if the recovery time of the SBR is in the order of or larger than the cavity round-trip time, the laser will not be mode-locked [6]. In that respect, usage of an SBR with a larger recovery time could also help with pure Q-switching. The SBR used in our study was optimized for mode-locking: some layers were low-temperature grown to induce defects and to achieve a relatively fast recovery time of around 20 ps. Ideally, the recovery times of AlGaAs-based absorbers could be designed to be in the few ns range, which could provide great benefit in achieving pure Q-switched operation. In short, we believe that, with proper engineering of the system, SBR Q-switched Cr:LiCAF lasers have the

potential to generate pulse widths and peak powers that are orders of magnitude better compared to what could be achieved in this initial study.

Acknowledgements UD acknowledge support from BAGEP Award of the Bilim Akademisi.

Funding Scientific and Technological Research Council of Turkey (TÜBİTAK, 119E264).

Compliance with ethical standards

Conflicts of interest The authors declare no conflicts of interest.

References

1. R. Paschotta, R.P.P.C. GmbH, *Encyclopedia of Laser Physics and Technology* (RP Photonics Consulting, Zürich, 2005)
2. K. Du, D. Li, H. Zhang, P. Shi, X. Wei, R. Diart, Electro-optically Q-switched Nd:YVO4 slab laser with a high repetition rate and a short pulse width. Opt. Lett. **28**, 87–89 (2003)
3. J.J. Degnan, Optimization of passively Q-switched lasers. IEEE J. Quantum Electron. **31**, 1890–1901 (1995)
4. A. Sennaroglu, Broadly tunable Cr^{4+}-doped solid-state lasers in the near infrared and visible. Prog. Quantum Electron. **26**, 287–352 (2002)
5. A.V. Podlipensky, V.G. Shcherbitsky, N.V. Kuleshov, V.P. Mikhailov, V.I. Levchenko, V.N. Yakimovich, Cr^{2+}:ZnSe and Co^{2+}:ZnSe saturable-absorber Q switches for 1.54-μm Er:glass lasers. Opt. Lett. **24**, 960–962 (1999)
6. K.J. Keller, F.X. Weingarten, D. Kärtner, B. Kopf, I.D. Braun, R. Jung, C. Fluck, N. Hönninger, J.A.A. Matuschek, Semiconductor saturable absorber mirrors (SESAM's) for femtosecond to nanosecond pulse generation in solid-state lasers. IEEE J. Sel. Top. Quantum Electron. **2**, 435–453 (1996)
7. S. Tsuda, W.H. Knox, S.T. Cundiff, W.Y. Jan, J.E. Cunningham, Mode-locking ultrafast solid-state lasers with saturable Bragg reflectors. IEEE J. Sel. Top. Quantum Electron. **2**, 454–464 (1996)
8. P.F. Moulton, Spectroscopic and laser characteristics of Ti:Al_2 O_3. JOSA B **3**, 125–133 (1986)
9. Walling, O.G. Peterson, H.P. Jenssen, R.C. Morris, E.W. Odell, Tunable alexandrite lasers. IEEE J. Quantum Electron. **16**, 1302–1315 (1980)
10. S.A. Payne, L.L. Chase, L.K. Smith, W.L. Kway, H.W. Newkirk, Laser performance of $LiSAIF_6$: Cr^{3+}. J. Appl. Phys. **66**, 1051–1056 (1989)
11. S.A. Payne, L.L. Chase, H.W. Newkirk, L.K. Smith, W.F. Krupke, $LiCaAlF_6$: Cr^{3+} a promising new solid-state laser material. IEEE J. Quantum Electron. **24**, 2243–2252 (1988)
12. L.K. Smith, S.A. Payne, W.L. Kway, L.L. Chase, B.H.T. Chai, Investigation of the laser properties of *s* Cr^{3+} : $LiSrGaF_6$. IEEE J. Quantum Electron. **28**, 2612–2618 (1992)
13. B.H.T. Chai, J.-L. Lefaucheur, M. Stalder, M. Bass, Cr:$LiSr_{0.8}$ $Ca_{0.2}$ AlF_6 tunable laser. Opt. Lett. **17**, 1584–1586 (1992)
14. J.F. Pinto, L. Esterowitz, G.H. Rosenblatt, Frequency tripling of a Q-switched Cr:LiSAF laser to the UV region. IEEE J. Sel. Top. Quantum Electron. **1**, 58–61 (1995)
15. J.F. Pinto, L. Esterowitz, Unstable Cr : LiSAF laser resonator with a variable reflectivity output coupler. Appl. Opt. **37**, 3272–3275 (1998)
16. U. Demirbas, Cr: Colquiriite Lasers: current status and challenges for further progress. Progress Quantum Electron. **68**, (year) 100227
17. S.A. Payne, L.L. Chase, L.K. Smith, B.H.T. Chai, Flashlamp-Pumped laser performance of $LiCaAlF_6$ Cr^{3+}. Opt. Quant. Electron. **22**, S259–S268 (1990)
18. F. Druon, F. Balembois, P. Georges, New laser crystals for the generation of ultrashort pulses. C.R. Phys. **8**, 153–164 (2007)
19. L.K. Smith, S.A. Payne, W.F. Krupke, L.D. DeLoach, R. Morris, E.W. O'Dell, D.J. Nelson, Laser emission from the transition-metal compound LiSrCrF6. Opt. Lett. **18**, 200–202 (1993)
20. V. Pilla, H.P. Jenssen, A. Cassanho, T. Catunda, Discrimination between thermal quenching of the fluorescence and Auger upconversion processes using thermal lens technique. Opt. Commun. **271**, 184–189 (2007)
21. U. Demirbas, Power scaling potential of continuous-wave Cr:LiSAF and Cr:LiCAF lasers in thin-disk geometry. Appl. Opt. **57**, 10207–10217 (2018)
22. V. Kubecek, R. Quintero-Torres, J.C. Diels, Ultralow-pump-threshold laser diode pumped Cr:LiSAF laser. Adv. Lasers Syst. **5137**, 43–47 (2002)
23. I.T. Sorokina, E. Sorokin, E. Wintner, A. Cassanho, H.P. Jenssen, R. Szipöcs, 14-fs pulse generation in Kerr-lens mode-locked prismless Cr:LiSGaF and Cr:LiSAF lasers:observation of pulse self-frequency shift. Opt. Lett. **22**, 1716–1718 (1997)
24. S. Uemura, K. Torizuka, Generation of 10 fs pulses from a diode-pumped Kerr-lens mode-locked Cr:LiSAF laser. Jpn. J. Appl. Phys. **39**, 3472–3473 (2000)
25. P.C. Wagenblast, U. Morgner, F. Grawert, T.R. Schibli, F.X. Kärtner, V. Scheuer, G. Angelow, M.J. Lederer, Generation of sub-10-fs pulses from a Kerr-lens mode-locked Cr^{3+}:LiCAF laser oscillator by use of third-order dispersion-compensating double-chirped mirrors. Opt. Lett. **27**, 1726–1728 (2002)
26. M. Stalder, B.H.T. Chai, M. Bass, Flashlamp pumped Cr:$LiSrAIF_6$ laser. Appl. Phys. Lett. **58**, 216–218 (1991)
27. J.K. Jabczyński, W. Zendzian, Z. Mierczyk, Z. Frukacz, Chromium-doped LiCAF laser passively Q switched with a V^{3+}:YAG crystal. Appl. Opt. **40**, 6638–6645 (2001)
28. Y.-K. Kuo, M.-F. Huang, M. Birnbaum, Tunable Cr^{4+}:YSO Q-switched Cr:LiCAF laser. IEEE J. Quantum Electron. **31**, 657–663 (1995)
29. C. S. Chen, Y. S. Zhang, J. W. Yu, J. Fang, S. H. Liu, Experimental study on dual wavelength and dual pulse Q-switched frequency doubling on a tunable Cr: LiSAF laser. Chinese Phys. Lett. **Volume**, (26)
30. D.E. Klimek, A. Mandl, Power scaling of a flashlamp-pumped Cr:LiSAF thin-slab zig-zag laser. IEEE J. Quantum Electron. **38**, 1607–1613 (2002)
31. B.C. Weber, A. Hirth, Efficient single-pulse emission with sub-microsecond duration from a Cr:LiSAF laser. Opt. Commun. **128**, 158–165 (1996)
32. B.C. Weber, A. Hirth, Presentation of a new and simple technique of Q-switching with a LiSrAlf(6): Cr3+ oscillator. Opt. Commun. **149**, 301–306 (1998)
33. F. Falcoz, K. Kerboull, F. Druon, F. Balembois, P. Georges, A. Brun, Small-signal gain investigations for a continous-wave diode-pumped Q-switched Cr:LiSAF laser. Opt. Lett. **21**, 1253–1255 (1996)
34. F. Balembois, F. Falcoz, F. Kerboull, F. Druon, P. Georges, A. Brun, Theoretical and experimental investigations of small-signal gain for a diode-pumped Q-Switched Cr:LiSAF laser. IEEE J. Quantum Electron. **33**, 269–278 (1997)
35. F. Balembois, F. Druon, F. Falcoz, P. Georges, A. Brun, Performances of Cr:$LiSrAlF_6$ and Cr:$LiSrGaF_6$ for continuous-wave

diode-pumped Q-switched operation. Opt. Lett. **22**, 387–389 (1997)
36. E. Beyatli, A. Sennaroglu, U. Demirbas, Self-Q-switched Cr:LiCAF laser. J. Opt. Soc. Am. B **30**, 914–921 (2013)
37. P. Pichon, A. Barbet, J.P. Blanchot, F. Druon, F. Balembois, P. Georges, LED-pumped alexandrite laser oscillator and amplifier. Opt. Lett. **42**, 4191–4194 (2017)
38. L. R. Jung Id Fau - Brovelli, M. Brovelli Lr Fau - Kamp, U. Kamp M Fau - Keller, M. Keller U Fau - Moser, M. Moser, Scaling of the antiresonant Fabry–Perot saturable absorber design toward a thin saturable absorber. Opt. Lett. **20**, (1995) 1559–1561
39. U. Demirbas, G.S. Petrich, D. Li, A. Sennaroglu, L.A. Kolodziejski, F.X. Kärtner, J.G. Fujimoto, Femtosecond tuning of Cr: Colquiriite lasers with AlGaAs-based saturable Bragg reflectors. JOSA B **28**, 986–993 (2011)
40. U. Demirbas, A. Sennaroglu, F.X. Kartner, J.G. Fujimoto, Comparative investigation of diode pumping for continuous-wave and mode-locked Cr^{3+}:LiCAF lasers. J. Opt. Soc. Am. B-Opt. Phys. **26**, 64–79 (2009)
41. U. Demirbas, I. Baali, D.A.E. Acar, A. Leitenstorfer, Diode-pumped continuous-wave and femtosecond Cr:LiCAF lasers with high average power in the near infrared, visible and near ultraviolet. Opt. Express **23**, 8901–8909 (2015)
42. G.J. Spühler, R. Paschotta, R. Fluck, B. Braun, M. Moser, G. Zhang, E. Gini, U. Keller, Experimentally confirmed design guidelines for passively Q-switched microchip lasers using semiconductor saturable absorbers. J. Opt. Soc. Am. B **16**, 376–388 (1999)
43. J.J. Zayhowski, P.L. Kelley, Optimization of Q-switched lasers. IEEE J. Quantum Electron. **27**, 2220–2225 (1991)
44. B. Braun, F.X. Kärtner, G. Zhang, M. Moser, U. Keller, 56-ps passively Q-switched diode-pumped microchip laser. Opt. Lett. **22**, 381–383 (1997)